AN EXPERIMENTAL INVESTIGATION ON AIR-SIDE PERFORMANCES OF FINNED TUBE HEAT EXCHANGERS FOR INDIRECT AIR-COOLING TOWER

by

Xueping DU[a], Yantao YIN[a], Min ZENG[a], Pengqing YU[a], Qiuwang WANG[a,*], Zhaoyi DONG[b], and Yitung CHEN[c]

[a] Key Laboratory of Thermo-Fluid Science and Engineering, Xi´an Jiaotong University, Shaanxi, China
[b] Beijing Longyuan Cooling Technology Co., Ltd, Beijing, China
[c] Department of Mechanical Engineering, University of Nevada, Las Vegas, Nev., USA

Original scientific paper
DOI: 10.2298/TSCI1403863D

A tremendous quantity of water can be saved if the air cooling system is used, comparing with the ordinary water-cooling technology. In this study, two kinds of finned tube heat exchangers in an indirect air-cooling tower are experimentally studied, which are a plain finned oval-tube heat exchanger and a wavy-finned flat-tube heat exchanger in a cross flow of air. Four different air inlet angles (90°, 60 °, 45°, and 30°) are tested separately to obtain the heat transfer and resistance performance. Then the air-side experimental correlations of the Nusselt number and friction factor are acquired. The comprehensive heat transfer performances for two finned tube heat exchangers under four air inlet angles are compared. For the plain finned oval-tube heat exchanger, the vertical angle (90°) has the worst performance while 45° and 30° has the best performance at small Re_{Dc} and at large Re_{Dc}, respectively. For the wavy-finned flat-tube heat exchanger, the worst performance occurred at 60°, while the best performance occurred at 45° and 90° at small Re_{Dc} and at large Re_{Dc}, respectively. From the comparative results, it can be found that the air inlet angle has completely different effects on the comprehensive heat transfer performance for the heat exchangers with different structures.

Key words: heat exchangers, air cooling, experimental investigation, heat transfer, flow resistance

Introduction

The available water resources become scarcer and scarcer. Thus the thermal power plant faces an unprecedented challenge because the water-cooling plays an important part on it. The use of air cooling systems in power plants is often justified where cooling water is not available or is very expensive [1]. Pistochini *et al*. [2] studied the water-use efficiency for alternative cooling technologies in arid climates. Their analysis results suggested that there existed viable alternatives for reducing the energy consumption and peak electricity demand that did not significantly increase the overall water use. Therefore, the large quantity of water can be saved if the air-cooling system is used in the industry or power plant, comparing with the ordinary water-cooling technology.

* Corresponding author; e-mail address: wangqw@mail.xjtu.edu.cn

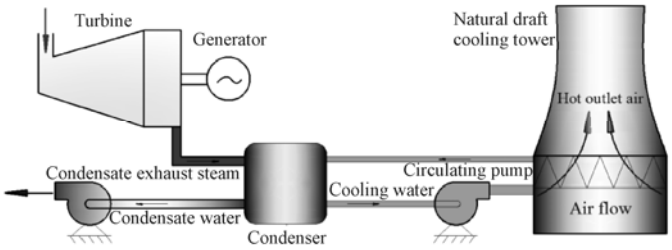

Figure 1. Schematic sketch of an indirect air-cooling system

An air-cooled heat exchanger (ACHX) is a device that facilitates the transfer of heat from a hot process fluid to ambient air [3]. It is found in the electronic industry, vehicles, air conditioning, and refrigeration plants as well as chemical and power plants where fluids at temperatures of approximately 60 °C or higher are to be cooled. A schematic sketch of an indirect air-cooling system is shown in fig. 1. As is well known, the finned tubes in ACHX of cooling towers are arranged in the form of an A-frame or delta to reduce the required land area [1]. A partial enlarged schematic view of the apex angle of the A-frame air-cooled radiator is shown in fig. 2. Four representative apex angles (α = 120°, 90°, 60°, and 45°) are simply drawn as an example. It can be noticed that much space will be saved if the apex angle becomes smaller in the radial direction of an air-cooling tower under the condition of the constant heat transfer area.

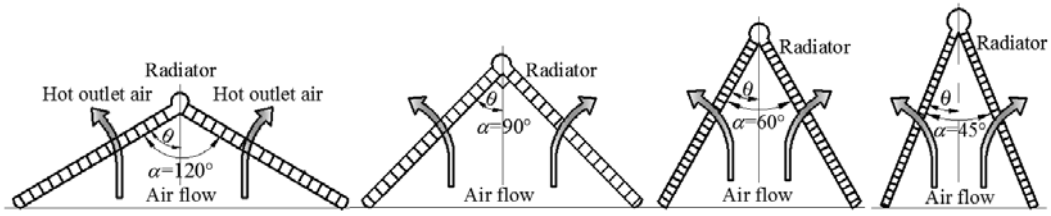

Figure 2. Partial enlarged drawing of apex angle (α) of air-cooling tower

Moreover, finned tube heat exchangers (FTHX) are used extensively in chemical and process industries for cooling purposes, especially in ACHX. ACHX is one of the very important components in the air-cooling tower. The thermal hydraulic performances for a louvered fin and elliptical tube heat exchanger [4] and some wavy finned flat tube heat exchangers with different geometry parameters [5, 6] were investigated experimentally and numerically, respectively. In particular, the authors' group [7-10] also studied FTHX with circular tube and different types of fins in recent years, using experimental, numerical and optimization methods. There are also many investigations [3, 11-14] on ACHX from different aspects. Meyer *et al.* [3, 11] researched ACHX experimentally and numerically, Kennedy *et al.* [12] investigated the heat exchanger inclination in forced-draught ACHX, and Yang *et al.* [13] studied the effects of ambient winds on the thermo-flow performances of indirect dry cooling system in a power plant, which supply a good reference for subsequent study of ACHX. Alinia Kashani *et al*. [14] investigated an ACHX unit from the point of thermal-economic optimization.

Although many researches on FTHX and ACHX are presented, there are few on the comprehensive performances and experimental correlations for finned oval-tube heat exchangers and flat-tube heat exchangers under different air inlet angles. Experimental studies are now underway in the authors' group to obtain the experimental correlations and comparative results of the comprehensive performance for different types FTHX under different air inlet

angles. Three finned oval-tube heat exchangers with carbon steel tubes and fins were experimentally studied under four air inlet angles by the authors' group [15, 16]. In order to continue the previous work to obtain more experimental correlations on different types of FTHX, two samples of FTHX with aluminum fins in the indirect air-cooling system will be studied under four air inlet angles in present experiment. Finally, the comprehensive heat transfer performances are compared based on the dimensionless correlations from the present experiment and three sets of identical criteria. The results given in the dimensionless formula of heat transfer and pressure drop of the air across the FTHX under different air inlet angles will be very useful for the engineers to design and apply the FTHX in the air-cooling tower.

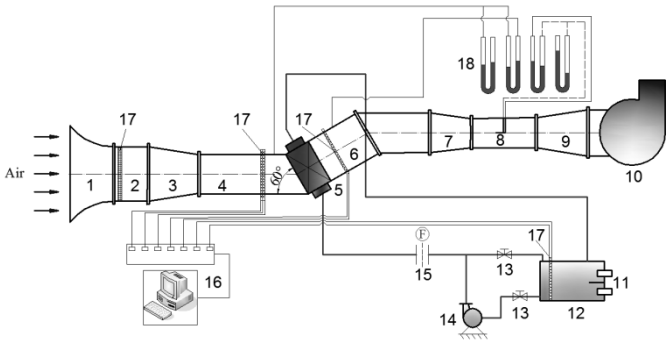

Figure 4. Schematic diagram of experimental system
1 – Entrance; 2 – Transition section; 3 – Contraction section; 4 – Straightening section; 5 – Test section; 6 – Straightening section; 7 – Contraction section; 8 – Flow metering duct; 9 – Expansion section; 10 – Blower; 11 – Electric heating rod; 12 – Water tank; 13 – Valve; 14 – Water pump; 15 – Turbine flowmeter; 16 – Data acquisition system; 17 – Thermocouples grid; 18 – U-tube manometer

Experimental system and procedure

In order to find the effects of the air inlet angle on the thermal hydraulic performance of FTHX in a cross flow of air, an experiment system is built with an open wind tunnel and water-cycling system, which is shown in fig. 3. It consists of two loops: air loop and hot water loop. The air loop is designed to blow air across the finned tube bundles of the FTHX, which are placed obliquely with different air inlet angles in the test section. The experimental system and procedure have already been described in detail in [15, 16], so the air loop, water loop, temperature measurements, pressure measurements, flow rates and data acquisition procedure can be found in [15, 16]. The experimental samples will be shown in detail as follows.

Two kinds of FTHX in a cross flow of air are studied in the present experiment. The two heat exchangers are both with

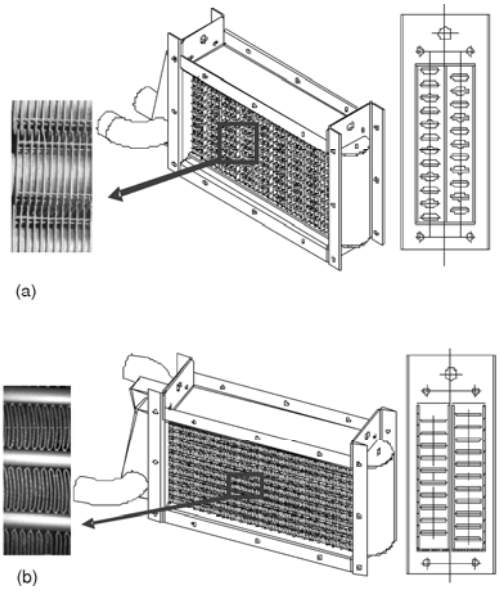

Figure 3. Schematic view of two test finned tube heat exchangers: (a) Plain finned oval-tube heat exchanger (PFOTHX), (b) Wave finned flat-tube heat exchanger (WFFTHX)

double rows of tubes and double tube-passes, but with different types of fins and tubes. The tested heat exchangers are schematically shown in fig. 4. In fig. 4(a), the heat exchanger is consisted of plain fins and oval-tubes, called the plain finned oval-tube heat exchanger (PFOTHX). The main difference between PFOTHX and the finned oval tube heat exchanger tested in [16] is the fin material. The fin material of the former is aluminum and the latter is carbon steel. The one in fig. 4(b) is made up of wavy fins and flat-tubes, called the wavy-finned flat-tube heat exchanger (WFFTHX). Both of the two heat exchangers with staggered tube layout are only test samples from the indirect air-cooling tower. Their main geometric parameters related to the two FTHX and air inlet angles are tabulated in tab.1. In the present experiment, all of the tubes are made from carbon steel, and fins are made from aluminum.

Table 1. Main geometrical dimensions of finned tube heat exchangers

	Main geometrical parameters					Air inlet angle
	a/b	F_l/F_w	F_l/F_h	F_l/F_S	P_l/P_t	θ°
PFOTHX	2.57	157.14	2.16	22	2.25	90, 60, 45, 30
WFFTHX	7.25	275	2.89	30.56	2.89	

Four different air inlet angles (90°, 60°, 45°, and 30°) are investigated in the present study. The air inlet angle is defined as the inclination angle between the air incoming flow direction and the minor axis of the oval-tube for PFOTHX, and the width direction of the flat-tube for WFFTHX, which is schematically illustrated in fig. 5, respectively. The air inlet angle of 60° in fig. 3 could be changed to other angles of 90°, 45° and 30° schematically depicted in fig. 5.

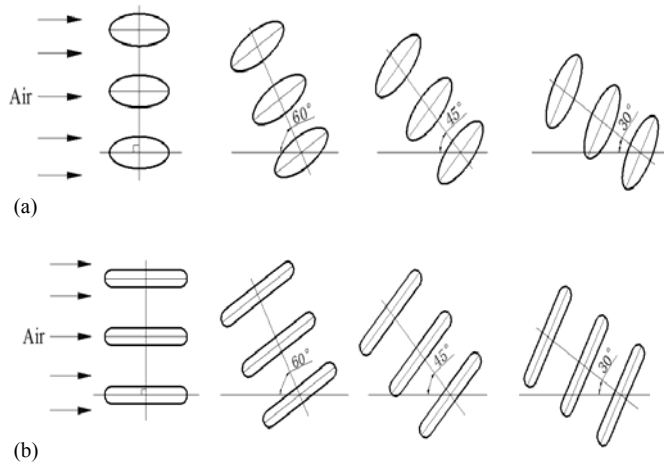

Figure 5. Schematic view of different air inlet angles of two heat exchangers: (a) Plain finned oval-tube heat exchanger; (b) Wavy finned flat-tube heat exchanger

Data reduction

The main purpose of the data reduction is to separate the air-side convection heat transfer coefficient from the overall heat transfer coefficient according to the experimental data. Then the dimensionless number of Nusselt number (Nu), friction factor (f) and the corresponding power-law correlations can be derived for each heat exchanger under each air inlet angle. The heat flow of the hot water, Φ_w, and the heat flow of the cold air, Φ_a, are calculated by the following equations, respectively:

$$\Phi_w = \rho_w q_w c_{pw} \Delta T_w \tag{1}$$

$$\Phi_a = m_a c_{pa} \Delta T_a \tag{2}$$

The overall heat transfer coefficient is calculated based on the total heat transfer area of the air side:

$$k = \frac{\frac{\Phi_a + \Phi_w}{2}}{\psi \Delta T_m A_o} \tag{3}$$

where ψ is the correction factor of temperature difference [17], and A_o the total heat transfer area of the air side, including the area of fins and base tubes.

The overall heat transfer resistance separation method is adopted to obtain the air-side convective heat transfer coefficient h_o. The overall heat transfer resistance can be defined as:

$$\frac{1}{kA_o} = \frac{1}{h_i A_i} + \frac{1}{2\pi\lambda L} \ln\frac{d_o}{d_i} + \frac{1}{h_o \eta_o A_o} \tag{4}$$

The heat transfer coefficient (h_i) of water side can be acquired through Gnielinski's formula [18]. The equivalent diameter for the oval tube is given as:

$$d = \frac{ab}{\sqrt{\frac{a^2 + b^2}{2}}} \tag{5}$$

where a is the length of the major axis, and b is the length of the minor axis. The hydraulic diameter of the flat-tube is taken as its equivalent diameter.

In eq. (4), the first two items of the right side can be computed, and only $h_o \eta_o$ is unknown. The efficiency η_o is the overall surface efficiency, which can be calculated from the equations shown in detail in [15]. Other detail data reduction process can be found in [15, 16].

The air-side heat transfer and pressure drop performances of the heat exchangers are presented in the following dimensionless forms (6), (7), and (8), where v_{max} is the maximum velocity at the minimum free flow area of the air side, and D_c is the fin collar outside diameter [19].

All the measurement instruments have been adjusted to verify the test results and methods before the experiment started to run. According to the uncertainty estimation methods of Kline and Mclintock [20], the maximum experimental uncertainty of the air-side Nusselt number is 8.26% for both PFOTHX and WFFTHX, and those of the friction coefficient are 11.98% and 18.30% for PFOTHX and WFFTHX, respectively. They are determined from the measuring equipments of fluid flow rate, pressure and temperature.

$$Nu = \frac{h_o D_o}{\lambda} \tag{6}$$

$$j = \frac{\mathrm{Nu}}{\mathrm{Re}_{D_c} \sqrt[3]{\mathrm{Pr}}} \tag{7}$$

$$f = \frac{2\Delta p}{\rho v_{max}^2} \frac{D_c}{l_f} \tag{8}$$

Results and discussion

Experimental results

Two kinds of FTHX (PFOTHX and WFFTHX) are tested under four air inlet angles (90°, 60°, 45°, and 30°), respectively. Then the corresponding Nusselt numbers and friction factors can be computed from the above data reduction procedures. Moreover, all the experimental data for the two tested heat exchangers under four air inlet angles were correlated separately.

The results are shown in figs. 6 and 7, where the scatters, solid lines and dashed lines represent the experimental data, the linear fitting lines in the logarithmic coordinates, and the corresponding error bars, respectively. In the present experimental study, the Reynolds number (Re_{Dc}) in the air-side varies from 1,650 to 13,500 for PFOTHX, and from 2,400 to 14,800 for WFFTHX. All the experimental correlations and comparison results for the same test heat exchanger under different air inlet angels are depicted as follows.

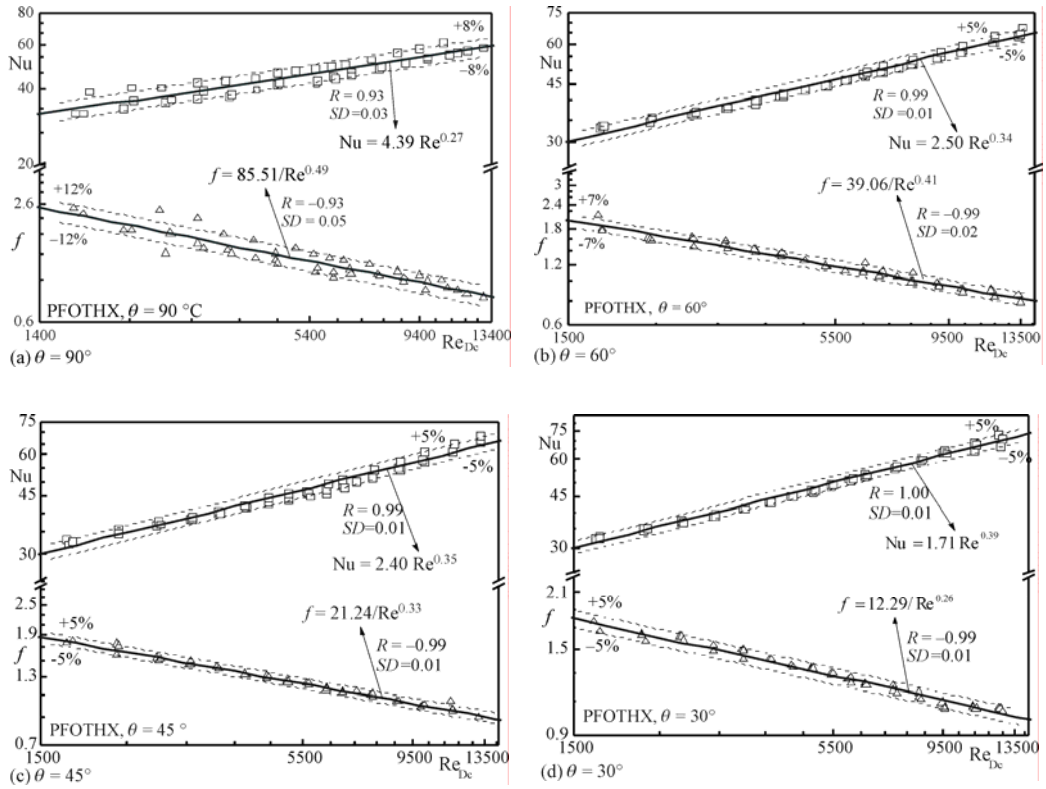

Figure 6. Correlations of Nu with Re_{Dc} and *f* with Re_{Dc} for PFOTHX

The correlations of Nu with Re_{Dc} and *f* with Re_{Dc} for PFOTHX under four different air inlet angles are shown in fig. 6. The heat transfer and flow resistance performances for WFFTHX under the four air inlet angles are given in fig. 7. All the experimental correlations of the coefficients are obtained by a linear fitting method in the logarithmic coordinates. From fig. 6 to fig. 7, it can be seen that most of the experimental data are within the range of the maximum error bars for each angle.

Moreover, the generalization capability of the fitting method is quantified in terms of the correlation coefficient (*R*), and standard deviation (*SD*) based on the experimental data and the fitted value according to the equations in ref. [15]. *R* and *SD* of the linear fitting in logarithmic coordinates in the present study are shown in figs. 6 and 7. *R* measures the data dependency during the experiment, which varies between –1 and 1. It means a close relationship when the absolute value of *R* is 1, while a random relationship when the absolute value of *R* is 0.

From figs. 6 and 7, it can be found that the slope of the linear fitting line for Nu is positive, so the value of R is greater than 0; while that for f is negative, so the value of R is less than 0. For SD, lower values are better. R reflects the scatter of the experimental data, while SD reflects the mean accuracy of the fitted experimental correlations. It can be seen that all the absolute values of the correlation coefficients of the linear fitting is more than 0.97, except that the one for PFOTHX at $\theta = 90°$ equals to 0.93, and the standard deviations are lower than 0.05, which indicate that all the experimental data used to obtain experimental correlations have very close relationships and high precision.

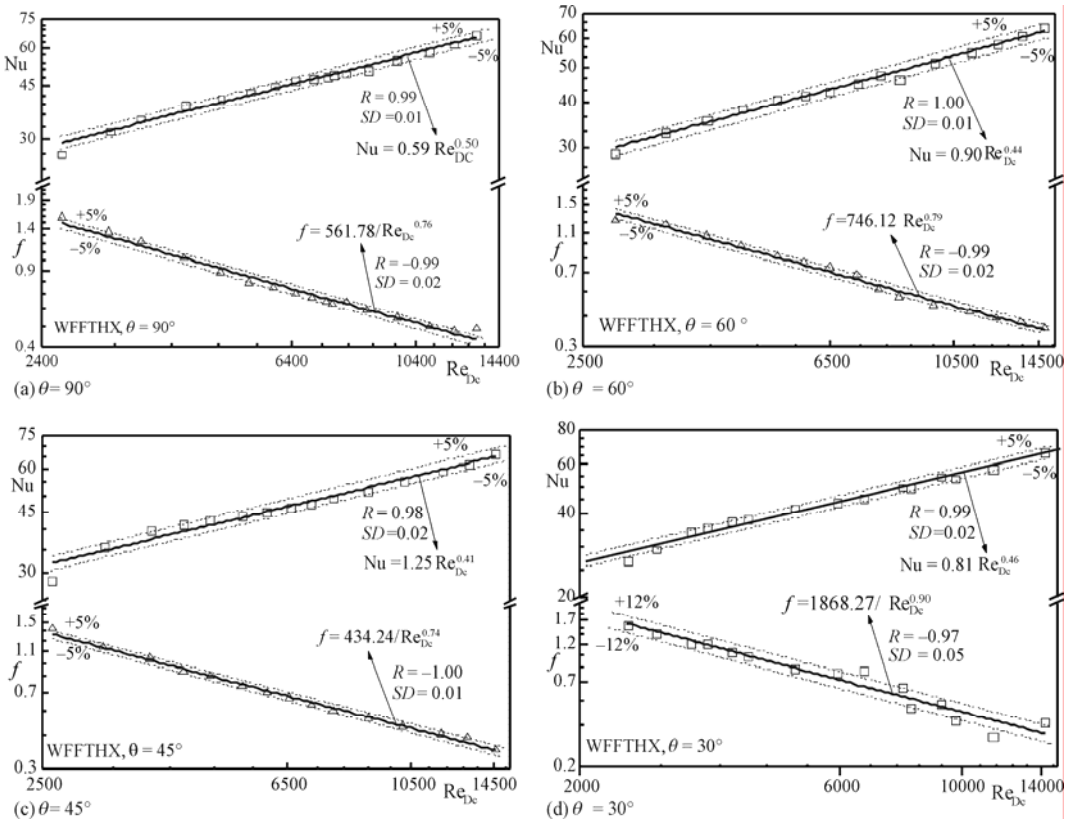

Figure 7. Correlations of Nu with Re_{Dc} and f with Re_{Dc} for WFFTHX

Comprehensive evaluation of heat transfer performance

As is well known to us, the enhancement of heat transfer is always accompanying with the increase of flow resistance. So the comprehensive heat transfer performances of the test heat exchangers under the four air inlet angles are evaluated to compare the air-side performance. Identical mass flow rate criteria (IMF), identical pressure drop criteria (IPD), and identical pumping power criteria (IPP) were successfully used [9, 21]. Thus these three identical criteria are also used to evaluate the comprehensive heat transfer performances of two heat exchangers under four different air inlet angles in the present study. The formulations of these identical criteria are given as follows [9, 15, 21].

(1) Identical mass flow rate criterion (IMF):

$$\left(\frac{\mathrm{Re}\,A_{\min}}{D_{\mathrm{c}}}\right)_{\mathrm{c}}=\left(\frac{\mathrm{Re}\,A_{\min}}{D_{\mathrm{c}}}\right)_{\mathrm{r}} \tag{9}$$

where the subscript "c" stands for the compared air inlet angles (60°, 45°, and 30°) and the subscript "r" means the reference air inlet angle (90°).

(2) Identical pressure drop criterion (IPD):

$$\left(\frac{f\,\mathrm{Re}^2}{D_{\mathrm{c}}^3}\right)_{\mathrm{c}}=\left(\frac{f\,\mathrm{Re}^2}{D_{\mathrm{c}}^3}\right)_{\mathrm{r}} \tag{10}$$

(3) Identical pumping power criterion (IPP):

$$\left(\frac{f\,\mathrm{Re}^3\,A_{\min}}{D_{\mathrm{c}}^4}\right)_{\mathrm{c}}=\left(\frac{f\,\mathrm{Re}^3\,A_{\min}}{D_{\mathrm{c}}^4}\right)_{\mathrm{r}} \tag{11}$$

According to the above three criteria and the experimental correlations, the ratio of the heat transfer rate between the compared air inlet angles and the reference air inlet angle may be calculated by eq. (12) with the same characteristic length, the constant thermal properties and the same temperature difference between the fluid and the wall:

$$\frac{\Phi_{\mathrm{c}}}{\Phi_{\mathrm{r}}}=\frac{\left[\mathrm{Nu(Re)}A_{\mathrm{o}}\right]_{\mathrm{c}}}{\left[\mathrm{Nu(Re)}A_{\mathrm{o}}\right]_{\mathrm{r}}} \tag{12}$$

where Nu(Re) represents the dimensionless correlation of Nusselt number *vs.* Reynolds number.

The comparative results of the comprehensive heat transfer performance of the four air inlet angles for PFOTHX and WFFTHX are shown in the logarithmic coordinates in fig. 8, respectively. The Reynolds number is taken as the abscissa and the heat transfer rate Φ_θ/Φ_{90} is the ordinate. The symbols $\theta = 60°$, $\theta = 45°$, and $\theta = 30°$ stand for the ratios of the heat transfer rate of 60°, 45°, and 30° to that of 90°, respectively. The dash line of $\Phi_\theta/\Phi_{90} = 1$ means the comprehensive performance of the air inlet angle at θ is the same as that of 90°. From fig. 8, it can be seen that based on the three criteria, the comprehensive performance of the two FTHX under the four air inlet angles are very different from each other. The performances of the two heat exchangers are analyzed as follows.

For PFOTHX, it can be seen clearly from fig. 8(a) that the ratios of heat transfer rates are more than 1 except a few points when the Reynolds number is too small, that is to say, the comprehensive heat transfer performance of the three inclined angles (60°, 45°, and 30°) is always superior to that of the vertical angle (90°) except a few individual experimental points with small $\mathrm{Re}_{\mathrm{Dc}}$. The performance of the inclined angles becomes much better and better than that of the vertical angle with the increasing of $\mathrm{Re}_{\mathrm{Dc}}$. So it can be approximately considered that the performance of 90° is the worst among the four air inlet angles, and that of 60° is the worst among the three inclined angles. It can be found that the slope of the line $\theta = 30°$ is larger than that for the other two inclined angles (60° and 45°), which is shown that the comprehensive heat transfer performance of 30° increase tremendously with the increase of $\mathrm{Re}_{\mathrm{Dc}}$. The comprehensive performance of 45° is better than that of 30° at small $\mathrm{Re}_{\mathrm{Dc}}$,, while that of 30° becomes

better than that of 45° when Re_{Dc} becomes higher than certain values under the three identical criteria. And the critical values of Re_{Dc} are about 4,790, 5,956, and 7,481 under IMF, IPP and IPD, respectively. In all, the comprehensive heat transfer performance of 90° is the worst while that of 45° is the best at small Re_{Dc}, and that of 30° is the best at large Re_{Dc} among the four angles for PFOTHX.

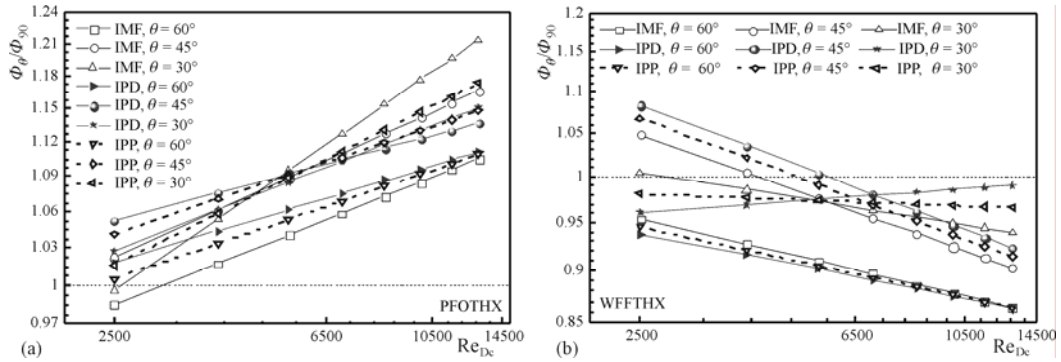

Figure 8. Heat transfer performance comparisons of different air inlet angles; (a) PFOTHX; (b) WFFTHX

For WFFTHX, it can be noticed from fig. 8(b) that the comprehensive heat transfer performance becomes worse and worse as the Reynolds number increases, except that of 30° under IPD criterion, which is very different from PFOTHX. That of 60° is the worst among the four angles. From the dash line of $\Phi_\theta/\Phi_{90} = 1$, it can be seen that the comprehensive performance of 45° is the best when the Reynolds number is small, while that of the vertical angle (90°) is the best when the Reynolds number exceeds the certain values based on the three identical criteria. The critical values of Re_{Dc} are about 4,196, 5,002, and 5,696 under IMF, IPP, and IPD, respectively. Between 45° and 30°, the comprehensive heat transfer performance of 45° is better than that of 30° at small Re_{Dc}, while that of 30° is better than that of 45° when the Reynolds number increases to the certain values based on the three criteria, which is the same as PFOTHX; the critical values of Re_{Dc} are about 5,868, 6,794 and 7,094 under IMF, IPP, and IPD, respectively. On the whole, the comprehensive heat transfer performance of 45° is the best at small Re_{Dc} and the case with 90° is the best at large Re_{Dc}, while the case with 60° is the worst for WFFTHX.

Moreover, to consider *j* and *f* factors simultaneously, the *JF* factor is shown in [22] as follows:

$$JF = \frac{\frac{j_c}{j_r}}{\sqrt[3]{\frac{f_c}{f_r}}} \tag{13}$$

This dimensionless number is a "the larger value the better" parameter, which means that the compared air inlet angles with larger *JF* factor have better comprehensive thermal-hydraulic performances. As can be seen from eq. (13), it is expected that the *JF* factor can be used to effectively evaluate the comprehensive performance of a heat exchanger under different air inlet angles since it includes both the *j* and *f* factor. The *JF* factors of different

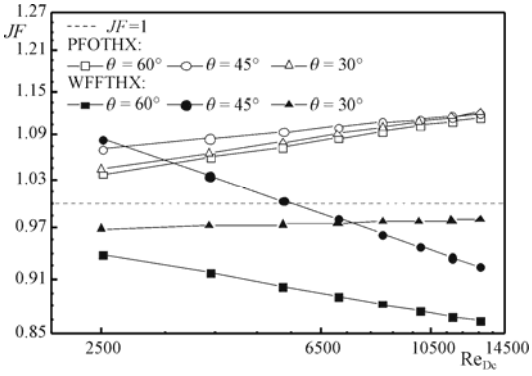

Figure 9. *JF* factor of different air inlet angles compared to reference angle

inclined air inlet angles (60°, 45°, 30°) compared to the reference air inlet angle (90°) according to the experimental results are shown in fig. 9. It can be found that, for PFOTHX, the value of the *JF* factor is larger than 1, which means that the comprehensive heat transfer performance of 90° is the worst and that of 45° and 30° is the best at small Re_{Dc} and large Re_{Dc}, respectively. For WFFTHX, the best comprehensive heat transfer performance occurs at 45° when the Reynolds number (Re_{Dc}) is small, while that occurs at 90° when the Reynolds number becomes larger than 5,736; the comprehensive performance of 60° is the worst. These findings agree well with the above results obtained by the three identical criteria.

As aforementioned, the comparative results of the comprehensive heat transfer performance show that the effects of the air inlet angle on the performance for two test FTHX are absolutely different. There is an obvious difference between the significant heat transfer enhancement of PFOTHX and the heat transfer deterioration of WFFTHX at large Re_{Dc} when the air inlet angle become smaller, which form a vivid contrast. This may be caused mainly by the following two aspects: (1) The different geometric structure of the two FTHX. For example, the fin efficiency of PFOTHX is very different from that of WFFTHX, which is 0.78 ~ 0.88 and 0.66 ~ 0.84 within the limits of the present experimental data, respectively. (2) The different effect of the air inlet angle on the flow and temperature fields. The velocity and temperature distributions are different due to the varied air inlet angle for the two test heat exchangers with different configurations.

Although the heat transfer performance is not always improved, the heat exchanger usually needs to be placed with an inclined angle to save space in the practical engineering applications, especially in the indirect air-cooling tower as shown in fig. 2. So the two FTHX under four air inlet angles are experimentally studied in the present experiment. For PFOTHX, the air inlet angle of 45° and 30° can be chosen directly according to the experimental results and practical application conditions. However, that for WFFTHX is not easy to choose because of the heat transfer deterioration with the decrease of the air inlet angle. So it needs to consider the comprehensive performance among the heat transfer, pump power, cost of investment, area saving and other practical conditions.

Conclusions

The air-side performances of two cross-flow FTHX (PFOTHX and WFFTHX) are experimentally studied under four air inlet angles (90°, 60°, 45°, and 30°). Then the comprehensive heat transfer performances are compared based on three identical criteria. According to the experimental results and the above comparative analysis, major conclusions of the present study are summarized as follows.

The experimental data are correlated to obtain the experimental correlations of Nu versus Re_{Dc} and f versus Re_{Dc} for the two FTHX under four air inlet angles. The correlation coefficients and standard deviations are acquired as an evaluation criterion for the accuracy of these formulas.

The comprehensive heat transfer performances for the two FTHX under four air inlet angles are evaluated based on three criteria (IMF, IPD and IPP), respectively. For PFOTHX, the comprehensive performance of the vertical angle (90°) is the worst while that of 45° and 30° is the best at small Re_{Dc} and at large Re_{Dc}, respectively; the critical values of Re_{Dc} are about 4790, 5956 and 7481 under IMF, IPP, and IPD, respectively. For WFFTHX, the worst performance occurred at 60°, while the best performance occurred at 45° and 90° at small Re_{Dc} and at large Re_{Dc}, respectively; the critical values of Re_{Dc} are about 4,196, 5,002, and 5,696 under IMF, IPP, and IPD, respectively.

Based on the obtained results and those from [15, 16], it can be found obviously that the influence of the air inlet angle on the air-side performance of FTHX with different structures is quite significant. So there must be an optimal air inlet angle to obtain the best comprehensive performance for a given FTHX obliquely used in an air-cooling tower, considering the heat transfer, pump power, space saving, environmental cost, investment cost, operating cost, and so on. And this kind of study can be carried out in the future according to the practical engineering application.

Nomenclature

A – area, [m^2]
a – outer length of the major axis of the oval-tube / flat-tube, [m]
b – outer length of the minor axis of the oval-tube / flat-tube, [m]
c_p – specific heat capacity, [$Jkg^{-1}K^{-1}$]
d – equivalent diameter of the oval-tube / flat-tube, [m]
D_c – fin collar outside diameter, ($= d_o+2\delta$), [m]
f – friction factor, [–]
F_h – fin height, [m]
F_l – fin length, [m]
F_s – fin spacing, [m]
F_w – fin width, [m]
h – heat transfer coefficients, [$Wm^{-2}K^{-1}$]
j – Colburn factor, [–]
JF – JF factor, [–]
k – overall heat transfer coefficient, [$Wm^{-2}K^{-1}$]
L – total length of tubes, [m]
l_f – fin length, [m]
m – mass flow rate, [kg s^{-1}]
Nu – Nusselt number, [–]
P_l – longitudinal tube pitch, [m]
Pr – Prandtl number, ($= c_p\mu/\lambda$)
P_t – transverse tube pitch, [m]
q – volume flow rate, [m^3 h^{-1}]
Re_{Dc} – Reynolds number, ($= \rho\, v_{max}\, D_c/\mu$)
ΔT – temperature difference, [K]
ΔT_m – log mean temperature difference, [K]
v_{max} – maximum air velocity, [m s^{-1}]

Greek symbols

α – apex angle of the above air-cooled radiator, [°]
δ – fin thickness, [m]
θ – air inlet angle, ($= \alpha/2$), [°]
λ – thermal conductivity, [$Wm^{-1}K^{-1}$]
μ – dynamic viscosity, [$kgm^{-1}s^{-1}$]
Φ – heat transfer rate, [W]

Subscripts

a air
i tube inside, water side
o tube outside, air side
w water

Acknowledgments

This work was supported by the China National Funds for Distinguished Young Scientists (No. 51025623), the Natural Science Foundation of China for International Cooperation and Exchange (No. 51120165002), and the Natural Science Foundation of China (No. 51276139).

References

[1] Kroger, D. G., *Air-Cooled Heat Exchangers and Cooling Towers, Vol. I*, PennWell Corporation,Tulsa, Okla., USA, 2004

[2] Pistochini, T., Modera, M., Water-use Efficiency for Alternative Cooling Technologies in Arid Climates, *Energy and Buildings, 43* (2011), 2-3, pp. 631-638
[3] Meyer, C. J., Kroger, D. G., Air-Cooled Heat Exchanger Inlet Flow Losses, *Applied Thermal Engineering, 21* (2001), 7, pp. 771-786
[4] Pooranachandran, K., *et al.,* Experimental and Numerical Investigation of a Louvered Fin and Elliptical Tube Compact Heat Exchanger, *Thermal Science*, On line first list, DOI: 10.2298/TSCI120220146P
[5] Dong, J. Q., *et al.,* Experimental Study on Thermal-Hydraulic Performance of a Wavy Fin-and-Flat Tube Aluminum Heat Exchanger, *Applied Thermal Engineering, 51* (2013), 1-2, pp. 32-39
[6] Du, X. Z., *et al*., Experimental Study on Heat Transfer Enhancement of Wavy Finned Flat Tube With Longitudinal Vortex Generators, *Applied Thermal Engineering, 50* (2013), 1, pp. 55-62
[7] Xie, G. N., *et al*., Parametric Study and Multiple Correlations on Air-Side Heat Transfer And Friction Characteristics of Fin-And-Tube Heat Exchangers with Large Number of Large-Diameter Tube Rows, *Applied Thermal Engineering, 29* (2009), 1, pp. 1-16
[8] Zeng, M., *et al*., Optimization of Heat Exchangers with Vortex-Generator Fin by Taguchi Method, *Applied Thermal Engineering, 30* (2010), 13, pp. 1775-1783
[9] Tang, L. H., *et al*., Experimental and Numerical Investigation on Air-Side Performance of Fin-and-Tube Heat Exchangers with Various Fin Patterns, *Experimental Thermal and Fluid Science, 33* (2009), 5, pp. 818-827
[10] Xie, G. N., *et al*., Application of a Genetic Algorithm for Thermal Design of Fin-and-Tube Heat Exchangers, *Heat Transfer Engineering, 29* (2008), 7, pp. 597 - 607
[11] Meyer, C. J., Kroger, D. G., Numerical Investigation of the Effect of Fan Performance on Forced Draught Air-Cooled Heat Exchanger Plenum Chamber Aerodynamic Behaviour, *Applied Thermal Engineering, 24* (2004), 2-3, pp. 359-371
[12] Kennedy, I. J., *et al*., Investigation of Heat Exchanger Inclination in Forced-Draught Air-Cooled Heat Exchangers, *Applied Thermal Engineering, 54* (2013), 2, pp. 413-421
[13] Yang, L. J., *et al*., Effects of Ambient Winds on the Thermo-Flow Performances of Indirect Dry Cooling System in a Power Plant, *International Journal of Thermal Sciences, 64* (2013), Feb., pp. 178-187
[14] Alinia Kashani, A. H., *et al*., Thermal-Economic Optimization of an Air-Cooled Heat Exchanger Unit, *Applied Thermal Engineering, 54* (2013), 1, pp. 43-55
[15] Du, X. P., *et al*., Experimental Study of the Effect of Air Inlet Angle on the Air-Side Performance for Cross-Flow Finned Oval-Tube Heat Exchangers, *Experimental Thermal and Fluid Science, 52* (2014), Jan., pp. 146-155
[16] Du, X. P., *et al*., Experimental Investigation of Heat Transfer and Resistance Characteristics of a Finned Oval-Tube Heat Exchanger with Different Air Inlet Angles, *Heat Transfer Engineering, 35* (2014), 6-8, pp. 703-710
[17] Wang, C. C., *Heat Exchanger Design* (in Chinese), Wunan Press, Taipei, China, 2003
[18] Kim, N. H., *et al*., Experimental Investigation on the Airside Performance of Fin-and-Tube Heat Exchangers Having Herringbone Wave Fins and Proposal of a New Heat Transfer and Pressure Drop Correlation, *Journal of Mechanical Science and Technology, 22* (2008), 3, pp. 545-555
[19] Wang, C. C., *et al*., Heat Transfer and Friction Characteristics of Plain Fin-and-Tube Heat Exchangers, part II: Correlation, *International Journal of Heat and Mass Transfer, 43* (2000), 15, pp. 2693-2700
[20] Kline, S. J., McClintock, F.A., Describing Uncertainties in Single-Sample Experiments, *Mechanical Engineering, 75* (1953), 1, pp. 3-8
[21] Wang, Q. W., *et al*., Experimental study of Heat Transfer Enhancement in Narrow Rectangular Channel With Longitudinal Vortex Generators, *Nuclear Engineering and Design, 237* (2007), 7, pp. 686-693
[22] Guo, L., *et al*., Influence of Geometrical Factors and Pressing Mould Wear on Thermal-Hydraulic Characteristics for Steel Offset Strip Fins at Low Reynolds Number, *International Journal of Thermal Sciences*, *46* (2007), 12, pp. 1285-1296

Paper submitted: December 18, 2013
Paper revised: January 24, 2014
Paper accepted: March 6, 2014